Uncovering the release of micro/nanoplastics from disposable face masks at times of COVID-19

Author names and affiliations:

Silvia Morgana[a,*], Barbara Casentini[b], Stefano Amalfitano[b]

[a] Institute for the Study of Anthropic Impact and Sustainability in the Marine Environment (IAS-CNR), Via della Vasca Navale, 00146 Rome, Italy

[b] Water Research Institute (IRSA-CNR), Via Salaria Km 29.300, 00015 Monterotondo (Rome), Italy

*Corresponding author.

E-mail address: silvia.morgana@ias.cnr.it

ABSTRACT

Wearing face masks is a fundamental prevention and control measure to limit the spread of COVID-19. The extensive use and improper disposal of single-use face masks are raising serious concerns for their environmental impact, owing to the foregone contribution to plastic water pollution during and beyond the pandemic. This study aims to uncover the release of micro/nanoplastics generated from the face mask nonwoven textile once discarded in the aquatic environment. As assessed by microscopy and flow cytometry, the exposure to simulated shear stress was proved to be effective in breaking and fragmenting face mask fabrics into smaller debris, including macro-, micro-, and nano-plastics. Even at low shear energy densities, a single mask could release in water thousands of microplastic fibers and up to 10^{11} submicrometric particles, mostly comprised in the nano-sized domain. By contributing to the current lack of knowledge regarding the potential environmental hazards posed by universal face masking, we provided novel quantitative data, through a suitable technological approach, on the release of micro/nanoplastics from single-use face masks that can threaten the aquatic ecosystems to which they finally end-up.

Keywords

Microfibers; Nanoplastics; Water pollution; Microscopy; Flow Cytometry

1. Introduction

The COVID-19 pandemic has been contrastingly but dramatically affecting human activities and natural environments at either global or local scale. Although lockdown measures are retained beneficial for the environmental quality especially in areas at high anthropogenic pollution levels (Saadat et al., 2020; Zambrano-Monserrate et al., 2020), such allowance for the environment is expected to be inherently provisional (Ragazzi et al., 2020). In particular, a daily increase of municipal solid wastes is raising serious concerns, owing to the overproduction and massive use of disposable personal protective equipment required against the primary aerial dispersal of SARS-CoV-2-containing droplets. At the beginning of the pandemic, the World Health Organization estimated that international demand for surgical masks, examination gloves, and protective screens stood respectively up to 89, 76, and 2 millions per month (World Health Organization, 2020). The use of masks has been made mandatory in most world regions, with such a high demand to rapidly overreach the local availability, distribution, and industrial production (Wu et al., 2020).

Specifically intended for single use, face masks protect against aerial contaminants, including pollen, chemical fumes and pathogens. The filtering capacity, and hence the level of protection, depends on materials used and the engineering design. Despite differences among brands, face masks are generally made by assembling different layers of a thin nonwoven textile: a waterproof outer layer to repel fluids, a middle filtering layer to prevent particles and pathogen-containing droplets from penetrating in either direction, an inner layer of absorbent materials to trap droplets from the user. The nonwoven fabric is obtained by bonding a mass of filaments together using heat, chemical, or mechanical means (spunbond and meltblown methods) to produce smooth, porous and highly durable sheets (Ding et al., 2020). Among the suitable plastic polymers, polypropylene is the most common used for assembling surgical mask, as it is relatively cheap and has low melt viscosity for easy processing (Chua et al., 2020).

Since the beginning of the COVID-19 pandemic, discarded face masks are reported to litter city streets, flow through sewage channels, float in sea water until reaching the bottom (Ardusso et al., 2021; De-la-Torre et al., 2021; Okuku et al., 2021), and risk evidences for local fauna were recently provided (Boyle, 2020; Gallo Neto et al., 2021). Under environmental conditions, plastic waste slowly degrade due to chemical, mechanical, and biological actions into micrometric and submicrometric plastic particles (Andrady, 2015; Frias and Nash, 2019). The smaller they are, the easier they can be ingested, accumulated and transferred by organisms along the food chain (Jiang et al., 2020). Ingestion of micrometric and submicrometric plastics is known to cause direct adverse effects (e.g., entanglement, suffocation) and to expose organisms to plastic-associated chemical and microbial agents with a prominent toxic and pathogenic potential (Sathicq et al., 2021; Vethaak and Leslie, 2016; Zhang and Xu, 2020).

Since the massive use of disposable face masks is likely to persist further beyond the current pandemic, there is urgent need to uncover all possible environmental repercussions. An increasing number of environmental studies are pointing to face masks as an emerging source of plastic pollution that will shortly add-up to the already critical situation (Patrício Silva et al., 2021; Prata et al., 2021; Sullivan et al., 2021). A preliminary assessment reported thousands of microfibers released from surgical masks following UV irradiation and mechanical stirring into artificial seawater (Saliu et al., 2021).

This study was intended to evaluate the potential release in water of micro/nanoplastics (MNPs) from the thin polypropylene (PP) textile used to assemble surgical face masks. More specifically, the aims were to (i) quantify the extent of plastic release from face mask fabrics at different levels of mechanical deterioration, (ii) characterize morphologies and size of released micro/nanoplastics across a wide dimensional range (i.e., from millimeters downward nanometers), (iii) provide evidence for potential implications of plastic pollution in water owing to the emerging disposable plastic wastes at the time of COVID-19.

In laboratory conditions, spunbond PP fabrics from face masks were exposed to increasing shear stress levels and the plastic particles released in water were assessed by microscopy and flow cytometry, with particular attention to control samples and pre-treatment procedures.

2. Material and methods

2.1. Experimental set-up: shear stress tests

The surgical face masks, purchased by GLF S.A.S. (Italy), consisted of 3 layers (i.e., inner, intermediate and outer) of polypropylene (PP) spunbond nonwoven fabric with a density of 30 g/m^2. Sixteen masks were cut with scissors to remove the external welding and the elastic ear loops. The white intermediate nonwoven spunbond PP layer (hereafter named fabric) was manipulated with metal tweezers, sized and weighed on a high precision analytical balance (XS BL 303 E-balance, China). The sampled fabric was then placed in a glass beaker containing 500 mL of ultrapure MilliQ water.

A kitchen chopper (type HDP40; Kenwood, UK), equipped with a rotating blender blade (radius 11 cm) and operating at the maximum power (800W), was used for a short-term shear damage process, specifically intended to mimic stress factors that mechanically deteriorate face masks once dispersed in the environment.

The shear tests were carried out on different fabrics at increasing times and corresponding energy densities (1 s = 1.6 kJ/L, 15 s = 24 kJ/L, 30 s = 48 kJ/L, 60 s = 96 kJ/L, 120 s = 192 kJ/L), as estimated from known parameters (i.e., chopper power, treatment time, treated water volume). Each test was repeated four times and included a preliminary control test performed with MilliQ water only (i.e., blank control). The beaker was carefully rinsed with MilliQ water (i.e., 5 times) in between each shear test to minimize external contamination. Homogenous water aliquots were collected by a glass Pasteur pipette while keeping the beaker under manual agitation after each test. Sample aliquots were then analyzed by the methods described in the following sections.

112 The treated fabrics were collected from the beaker with tweezers, gently squeezed, and
113 weighed after overnight drying at 40°C. The percentage of deterioration was measured in
114 terms of weight loss, as follows:
115
116 (W_1-W_2/W_1) *100
117
118 where W_1 is the dry weight of the intact fabric (i.e., before blending), W_2 is the dry weight of
119 the treated fabric (i.e., after blending).
120
121 *2.2. Optic and epifluorescence microscopy for fabric texture characterization and*
122 *microplastics analyses*
123 The nonwoven fabric texture and filament web were inspected by a flat-field achromatic 40x
124 magnification lens, mounted on a cell phone, with an optical resolution of approx. 2 µm
125 (Tinyscope; https://www.tinyscope.com/ Wuhan, China). Upon calibration through a
126 micrometric scale, a representative number of pictures (2.16 × 3.84 mm) were taken on intact
127 and shear-damaged areas of dried fabrics to assess (i) density (i.e., number per unit area) and
128 morphology (i.e., shape and size) of the breathability-related holes, (ii) thickness and integrity
129 of PP filaments, with the help of digital magnification (up to 300×).
130 The occurrence of microplastics (MPs) released in water upon the shear tests (i.e., 16
131 samples) was assessed by an optical stereomicroscope (STEMI SR, Zeiss, Weet, Germany).
132 Homogenous water aliquot (5 mL) was placed in a glass Petri dish and carefully inspected
133 across a magnification range from 10× to 50×. For each aliquot, the mostly recurrent particle
134 types (i.e., homogeneous fibers excised from the filament web) were visually sorted and
135 measured (Morgana et al., 2018). This procedure was repeated until a minimum of 50 MPs
136 were counted for each tested fabric (Brandon et al., 2016). The visual identification allowed

the detection of MPs with a minimum size of 100 µm (hereafter named >100 µm). The final abundance value was expressed as items/m^2 and items/g of fabric.

The LED microscope CyScope HP (Sysmex Partec Italia s.r.l.), employing transmitted light and fluorescence detection and equipped with UV and green excitation/emission sets, was used to verify the occurrence of micrometric and sub-micrometric particles and to check for their autofluorescence level. Briefly, sample aliquots (20 µL) were placed onto wells of a chambered slide (10-well epoxy-coated slides with well diameter of 6.7 mm – Thermo Scientific, Germany) and inspected at 400× (in air) and 1000× (mounting coverslip and using an immersion oil objective lens).

2.3. Flow cytometry for micro/nanoplastic counting and characterization

After the shear tests, sample aliquots (1 mL) were collected from all samples (including controls) and transferred into 2-mL Eppendorf tubes. Each aliquot was immediately treated with H_2O_2 30% (1:1 dilution), incubated at 40°C and analyzed at 24 h from sampling. This pre-treatment was applied to limit the occurrence of particulate organic matter that could interfere with plastic particle counting (Bessa et al., 2019).

All sample aliquots were analyzed using a bench-top flow cytometer (A50-Micro; Apogee Flow Systems, Hertfordshire, UK), equipped with a solid-state UV laser (375 nm, 20 mV) and a blue laser (488 nm, 20 mV). According to the system specifications from the manufacturer, this flow cytometer is suitable to detect and quantify all suspended particles approximately from 0.08 µm to 100 µm, based on the light scatter signals and following a direct calibration with commercial solutions containing fluorescent beads at known size.

In this study, we used polystyrene yellow-green fluorescent calibration microspheres (Sub-micron Size Reference Kit, 10^6 green fluorescent beads/mL, Invitrogen™, F13839), with 5 different nominal diameters (0.1 µm, 0.2 µm, 0.5 µm, 1.0 µm, 2.0 µm), as reference reagents

to arrange voltages of photomultipliers (PMTs), threshold values, and the size-dependent gating strategy on histogram and density plots.

The forward light scatter (FSC) was set at the lowest voltage (PMT = 200 V) to maximize the size range of detectable particles, while the side light scatter (SSC) was set at 350 V to obtain a better resolution for sizing submicrometric particles. PMTs on blue (430 - 470 nm), green (530/30 nm), orange (590/35), and red (>610 nm) fluorescence channels were set at 410 V for the detection of fluorescent events.

The analysis of plastic particles was performed exclusively under UV excitation on all samples (i.e., 44 runs including controls). Upon the analysis of ultrapure MilliQ water, thresholding was set on the SSC channel and adjusted to move the background and instrumental noise below the first decade. Samples were run at low flow rates to keep the number of cytometric events below 1000 events/s and all acquired signals were plotted using the same settings. Given the comparable refractive indexes of polystyrene and polypropylene (Shackelford, 2000) and according to the SSC peak signals (SSC-H ±10%) of the calibration microspheres, we designed specific gates onto log-scaled cytograms for 4 size classes of plastic particles. By following the definition proposed by Gigault et al. (Gigault et al., 2018), we identified the classes "> 1.0" (MPs with a nominal diameter ≥ 1.0 µm but smaller than then maximum analytical size of 100 µm), "0.5-1.0" (NPs ≥ 0.5 µm but < 1 µm), "0.1-0.5" (NPs ≥ 0.1 µm but < 0.5 µm), "< 0.1" (NPs < 0.1 µm but larger than then minimum analytical size) (Figure S1). A log-log density plot of signal peak versus area (i.e., FSC-H vs FSC-A) was used to visualize and assess the occurrence of non-spherical particles. The deviation from a linear relation between the two signal values allowed discriminating spherical (FSC-H = FSC-A) vs non-spherical particles (FSC-H < FSC-A).

To assess the occurrence of microbial cells that could contribute to an overestimation of submicrometric particles by interfering across the targeted size range, the Total Cell Counts (TCC) were determined under blue laser excitation on the third untreated subset of sample

188 replicates. Following a consolidated protocol described elsewhere, aliquots (300 µL) were
189 stained for 10 min in the dark at room temperature by SYBR Green I (1:10000 dilution; Life
190 Technologies, code S7563). Thresholding was set at 10 fluorescence units on the green
191 channel and microbial cells were quantified by their signature on the density plot of the side
192 scatter vs the green fluorescence signals (Amalfitano et al., 2018).
193 The volumetric absolute counting, expressed as events per mL (i.e., items/mL, cells/mL), and
194 all supportive cytometric data (e.g., median values of FSC and SSC, percentage of non-
195 spherical particles, percentage of autofluorescent particles) were extracted from designed
196 gates by using the Apogee Histogram Software (v89.0). The .fcs files are freely available at
197 the Flow Repository identifier: https://flowrepository.org/xxx.
198
199 *2.4. Data analysis*
200 All particles released in water after each shear test were referred to size and weight of the
201 treated PP fabric, thus expressing data respectively as items/m^2 and items/g of PP fabric.
202 Moreover, the relative contribution of the 5 size classes to the total retrieved particles was
203 calculated and related to the shear test efficacy (i.e., particle concentration or weight vs
204 applied energy density or percentage of weight loss after treatment). Depending on the
205 observed prevailing particle morphologies detected by either microscopy or flow cytometry,
206 the mean volume (µm^3) was calculated by considering particles as spheres or as filaments, as
207 follows:
208
209 Microsphere mean volume $V = 4/3 \times \pi \times (D/2)^3$
210 Filament mean volume $V = (D/2)^2 \times \pi \times L$
211
212 Where D is the nominal diameter and L the length of microscopy-detected particles. An
213 approximate mean diameter was used for cytometry-detected particles within the size classes

214 defined according to the calibration beads. The mean volume was then multiplied by the
215 particle counts in each class and by the density of PP (900 kg/m^3) to estimate their
216 contribution to the total mass.
217 The correlation between the release of particles and the percentage of fabric deterioration was
218 carried out using the Spearman's rho test. As previously invoked to explain the observed size
219 distributions of plastics in aquatic environments (Brown and Wohletz, 1995; Timár et al.,
220 2010), the sigmoid Weibull and lognormal distributions were applied to empirically model the
221 plastic release, fragmentation, and agglomeration processes that may have occurred during the
222 shear tests.
223
224 *2.5. Quality control*
225 Quality control was checked by adopting all precautions recommended to limit the
226 overestimation of microplastic counts, including wearing of cotton gloves and laboratory
227 coats. Glassware was thoroughly cleaned with MilliQ water. To check that no airborne
228 contamination occurred in the laboratory, a blank control dish was left open on the lab bench
229 and inspected at the optical microscope during the experiments (Wesch et al., 2017).
230 Moreover, when approaching the instrumental limits for the detection of nanoplastics,
231 contamination may become relevant, therefore the aspecific signals detected on the blank
232 control (i.e., at each preliminary shear test performed with ultrapure MilliQ water only) were
233 subtracted from the concentration values of the target particles per each of the 4 size classes.
234
235 **3. Results**
236 *3.1. Deterioration of PP fabric at increasing shear stress intensities*
237 Before treatments, all the 16 nonwoven PP fabrics showed comparable size (approx. 135 x
238 130 x 0.125 mm), weight (549 ± 54 mg), and an intact texture with well-shaped rhomboid
239 holes (approx. 0.6 mm^2), placed at a fixed distance (0.4 holes/mm^2) across a tangled web of

PP filaments (20-30 μm in thickness). At higher shear stress intensities, larger areas of deterioration were found by visually inspecting the PP fabrics, with increasingly occurring shear-damaged holes and filaments resulting into a fuzzier fabric texture (Figure 1). The water temperature raised from 17.5 °C to 21.0 °C (at the longest treatment time of 120 s). A significant positive linear relation was found between the tissue deterioration level (% of weight loss) and the shear energy density (kJ/L) at increasing treatment times ($n = 16$; $r = 0.695$, $p = 0.003$) (Table 1).

3.2. Release of plastic particles from treated PP fabrics

The release in water of fabric fragments and plastic particles, excised from the web of PP filaments, was observed (Figure 2). The released MPs >100 μm were fiber-like, with few large fabric pieces (>5 mm, not considered in the counting). Observation at optic microscope showed an increase in the formation of MPs along with the shear energy density and in the percentage of fabric deterioration across the treatment time from 1 s (mean ± sd = $0.3 \pm 0.1 \times 10^5$ items/m^2 of treated fabric, corresponding to $0.9 \pm 0.2 \times 10^3$ items/g of PP) to 120 s ($2.8 \pm 0.5 \times 10^5$ items/m^2; $8.7 \pm 1.5 \times 10^3$ items/g of PP).

Smaller, mostly spherical, and abundant particles were visually spotted by microscopy and quantified by flow cytometry. A significant reduction of total counts was obtained by subtracting the unspecific signals detected in the blank controls at each shear test and size class (55.6 ± 19.6%). Moreover, following the SYBR Green staining protocol, the occurrence of microbial contamination was negligible and did not bias the particle counts within the size classes (approx. 10^3 cells/mL).

The mean value of total released particles was $2.1 \pm 1.4 \times 10^{11}$ items/m^2 of treated fabric, corresponding to $7.0 \pm 4.9 \times 10^9$ items/g of PP. The release of particles increased with energy density and fabric deterioration across treatment times from 1s ($7.6 \pm 4.6 \times 10^9$ items/m^2) to

30s ($3.9 \pm 1.2 \times 10^{11}$ items/m^2), with a slight but not significant reduction afterward (60s = $2.8 \pm 0.5 \times 10^{11}$ items/m^2; 120s = $2.1 \pm 0.7 \times 10^{11}$ items/m^2).

By plotting the forward scatter peak and area signals (FSC-H vs FSC-A), the large majority of detected particles were spherical (FSC-H = FSC-A; > 99% of items within <0.1 μm and 0.1-0.5 μm size classes) and non-fluorescent (blue channel < 10 fluorescence units). However, in 0.5-1.0 μm and >1.0 μm size classes, the occurrence of non-spherical particles increased with treatment time (FSC-H < FSC-A; >20% of total items at 120s), along with the percentage of blue autofluorescent items (i.e., 65.5 ± 24.3% of total items in the >1.0 μm size class).

In numerical terms, particles distribution was dominated by 0.1-0.5 μm size class particles (78.9 ± 6.5 % of total items), followed by nano-sized particles (<0.1 μm = 20.5 ± 7.5 %). Conversely, in terms of weight, the larger microfibers and micrometric particles contributed the most to the total retrieved mass (>100 μm = 64.3 ± 24.7%; >1.0 μm = 26.1 ± 18.4% of total mass) (Figure 3).

Despite higher shear energy densities reflected greater fabric deterioration and particle release in water, the occurrence of MPs >100 μm followed a sigmoidal increase over treatment and did not correlate with the log-normal release of particles belonging to smaller size classes. Regardless the total counts, the patterns of particle release were different among the size classes (Figure 4).

4. Discussion

This study was entailed to assess the potential release in water of micro/nanoplastics generated from single-use face masks once discarded in the environment. By adopting an experimental setup similar to that presented by Enfrin et al. (Enfrin et al., 2020), a two-blade impeller was used at increasing times to induce the deterioration of face mask nonwoven

289 textile with the release and fragmentation of micro/nanoplastics in water at low levels of
290 mechanical stress.
291 The nonwoven fabric texture with large tiny-filament intervals within each layer, on the one
292 hand, guarantees face mask quality standard (Chua et al., 2020), on the other hand, it makes
293 the filtering PP filament web vulnerable to mechanical damage. After gentle agitation in
294 deionized water, plastic face masks were found to leach microfibers, along with associated
295 heavy metals and organic compounds (Sullivan et al., 2021). Microfiber generation was also
296 demonstrated upon breathing simulation tests (Li et al., 2021), thus raising concern for their
297 potential inhalation and ingestion risk.
298 Given the rapid advancement of plastic detection methods and the relative simplicity in
299 designing deterioration tests under controlled laboratory conditions (Lambert and Wagner,
300 2016; Mattsson et al., 2021; Song et al., 2017), the experimental approach is likely to
301 represent a fundamental first step to provide reproducible evidences on the fate and potential
302 implications of plastic materials ending-up into aquatic systems. Here, we intended to mimic
303 the action of external mechanical stress forces that discarded face masks can encounter in the
304 environment. The applied energy densities (i.e., 1.6 - 192 kJ/L) were significantly lower than
305 that used for breaking down large plastics (11 MJ/L applied on polystyrene lids and styrene
306 foam (Ekvall et al., 2019)), and in line with values reported at wastewater treatment plants
307 (10-150 kJ/L (Enfrin et al., 2020)).
308 The mechanical deterioration over prolonged time scales was reported to primarily contribute
309 to the fragmentation of plastic debris across the transfer from land to water. On land, frictional
310 stresses generated by abrasion with the road surface can easily overcome the limiting strength
311 of the nonwoven textile, resulting in micro-cutting of the face mask fabric (Zhang et al.,
312 2021). Similarly, the mechanical degradation of PP textile can be promoted by collision with
313 rocks and sands caused by e.g. wind, waves, and tides, which are estimated to generate energy
314 densities of 0.5 - 50 J/m^3 of air/water (Layton, 2008). In natural and engineered aquatic

systems, face mask deterioration will largely depend on local hydrodynamic conditions, with an estimated time of tens to hundreds years for the full decomposition of plastic components (Chamas et al., 2020). Precipitation, weathering, surface runoff, water flow acting on river bed, bottom currents upon the sea floor, waves-rocks interaction, but also the transport through pipes, drains, and water treatment steps, are reported as the main routes driving plastic transfer and mechanical deterioration (Duan et al., 2021; Kane et al., 2020; Zhang et al., 2021).

In this study, a consistent number of micro/nanoplastics was immediately released into the aquatic medium following the first second of treatment, and then continued with different trends according to particle size and shape. Although first evidences on plastic fiber release from face mask are provided (Saliu et al., 2021; Sullivan et al., 2021), there is still a lack of knowledge on this potential environmental threat and its contribution to microfiber presence in environment (Xu and Ren, 2021). The generation of microplastic fibers as a function of mechanical stress intensity has been mostly investigated after laundry operation of synthetic textile and clothing, reporting that increasing temperature, wash duration, sequential washing, and the use of detergents promoted the release of microfibers. A large body of recent literature indicates that laundering clothing is a significant point source for emissions of microplastic fibers to oceans (Cesa et al., 2020; Hernandez et al., 2017; Napper and Thompson, 2016; Zambrano et al., 2019). De Falco et al. (De Falco et al., 2018) found that the number of microfibers increased from $1.6 \pm 0.5 \times 10^2$ items/g of fabric when washed with water alone to $1.3 \pm 0.2 \times 10^3$ items/g fabric using liquid detergent, and to $3.5 \pm 0.7 \times 10^3$ items/g of fabric using powdered detergent. Yang et al. (Yang et al., 2019) found significant differences when laundering different fabrics at increasing temperature, with a maximum of $7.5 \pm 0.1 \times 10^4$ microfibers/m^2 released after washing at 60 °C.

A major concern is that plastic microfibers can be fragmented into thousands of nano-sized particles that are more persistent and difficult to be detected (Henry et al., n.d.). Apparently

following a fragmentation process, we found a general prevalence for spherical nanoparticles in the size class 0.1-0.5 µm, followed by the smallest size class (<0.1 µm) at higher energy densities. Although further confirmations are needed, the fragmentation rate of face mask fabrics can be higher than that determined in this study, since several complex factors may co-occur in the environment, thus accelerating the overall plastic deterioration (Julienne et al., 2019). Moreover, the total release of micro/nanoplastics was not linearly correlated with weight loss and deterioration of the treated fabrics, but rather followed an asymptotic curve at increasing shear stress. These findings could point either to technical detection issues, since large fabric fragments (i.e., > 5 mm) and small nanoparticles (i.e., < 80 nm) were not reliably quantified, or to the density-dependent aggregation/agglomeration of the newly-formed nanoplastics, as also reported in experimental and field studies (Singh et al., 2019). Both fragmentation and agglomeration processes could be evoked to explain the different release trends observed between the target particle size classes.

Notably, blue autofluorescence signals were detected for micrometric particles (>1.0 µm) and decreased with size. Some plastic particles were reported to show detectable levels of autofluorescence, after excitement by near UV or visible radiation (e.g., polycarbonate, poly(methyl-methacrylate), poly(dimethylsiloxane), cyclo-olefin copolymer) (Kaile et al., 2020; Piruska et al., 2005), which can be amplified upon specific thermal/chemical treatments (Monteleone et al., 2021; Young et al., 2013). Overall, such phenomenon has inherent implications in particle detection, and the autofluorescence properties, coupled with secondary staining techniques, deserve to be further explored to improve the identification and characterization of a large fraction of the micro/nanoplastic pool (Kaile et al., 2020).

Among the numerous gaps affecting the current knowledge on micro/nanoplastic research, including environmental presence, transport pathways, adsorption of contaminants, and even the definition of size limits (Frias and Nash, 2019), there is not a general consensus on detection methods (Caputo et al., 2021). We showed the potential application of flow

cytometry for detecting micrometric and submicrometric plastic particles. Yet rarely considered for non-biological targets, this technology has been successfully applied to detect small plastic particles in aquatic media (Bringer et al., 2020; Kaile et al., 2020; Le Bihanic et al., 2020), with performances comparable to those showed by other more established analytical techniques (e.g., dynamic light scattering, nanoparticle tracking analysis) (Caputo et al., 2021). FCM was suitable for detecting homogenously distributed particles in liquid suspensions, albeit challenging when applied to environmental and biological complex matrices. Therefore, particular attention has to be directed toward removing all potential sources of particle quantification bias. Here, the subtraction of false positive signals detected in blank samples (55.6 ± 19.6% of total counted items) confirmed the fundamental need for quality controls, especially when working within the nano-size range. Taking advantage from the available literature on MNPs (Enfrin et al., 2020; Kaile et al., 2020; Prata et al., 2021), we carefully included a series of steps (i.e., a thoroughly washing of all FCM fluidics between each treatment, sample digestion in H_2O_2) to avoid particle count overestimation. For the purpose of this experimental study, FCM was proved to be a flexible, nearly real-time (i.e., time to results < 20 minutes from sampling) and reliable (i.e., thousands of events counted per second) technology to quantify plastic particles released from face masks across a wide dimensional range.

After treating the nonwoven PP fabrics at the lowest mechanical stress (i.e., 1.6 kJ/L, comparable to wind energy on a moderately windy day or slow tidal movement), a single 3 layers-face mask may generate 2×10^3 microfibers (> 100 µm), as comparably reported in previous experimental tests (Saliu et al., 2021), and up to 7×10^8 submicrometric particles. Notably, the mechanical deterioration of just 1% of the fabric layers (i.e., 96 kJ/L, easily reached within wastewater treatment plants or upon few months of exposure to environmental stress factors) could result into the release in water of approximately 20 mg of micro/nanoplastics per face mask.

Since global estimates reported that more than 10 million masks can be discarded monthly in the environment with a total weight of 30-40 tons (Adyel, 2020), this may translate into 10^{10} microfibers and 10^{15} micro/nanoplastics entering the aquatic ecosystem per month. Such extrapolation of experimental data must be used with due caution, but it clearly suggests that universal face masking will likely add further burden to the current plastic pollution level in water. As nonwoven textiles used for disposable protective equipment and sanitary products (e.g., wet wipes and sanitary towels) are emerging as potential new sources of micro/nanoplastics (Ó Briain et al., 2020; Shruti et al., 2020), it is deemed critical to include face masks in plastic pollution research for a more accurate projection of the global plastic budget.

5. Conclusions

With the universal necessity of wearing face masks to fight the COVID-19 pandemic, it is urgent to elucidate the environmental fate and potential implications of the inappropriate disposal of single-use plastic wastes. By mimicking realistic deterioration conditions, our experimental results revealed that a consistent high number of micro/nanoplastics can be promptly released from a single mask into the aquatic environment. The release pattern of micro/nanoparticles appears a critical yet undervalued circumstance that should be reconsidered into harmonized test protocols and analytical procedures for assessing the liability of ubiquitous plastic-based materials to mechanical deterioration, fragmentation, and agglomeration processes in view of a tailor-made management strategy for end-of-life plastics.

Acknowledgements

The Authors thank Massimo Sanchez and Valentina Tirelli of the Flow Cytometry Area (Core Facilities, Italian Institute of Health - ISS) for providing technical support and valuable advice

on the interpretation of flow cytometric data. The experimental activities were partly supported by the projects GO-FOR-WATER (ERA-NET FLAG ERA III, n. 825207) and GRAPHIL (GrapheneCore3-H2020-SGA-FET-GRAPHENE, n. 881603).

References

Adyel, T.M., 2020. Accumulation of plastic waste during COVID-19. Science (80-.). 369, 1314–1315. doi:10.1126/science.abd9925

Amalfitano, S., Fazi, S., Ejarque, E., Freixa, A., Romaní, A.M., Butturini, A., 2018. Deconvolution model to resolve cytometric microbial community patterns in flowing waters. Cytom. Part A 93, 194–200. doi:10.1002/cyto.a.23304

Andrady, A.L., 2015. Persistence of Plastic Litter in the Oceans, in: Marine Anthropogenic Litter. Springer International Publishing, Cham, pp. 57–72. doi:10.1007/978-3-319-16510-3_3

Ardusso, M., Forero-López, A.D., Buzzi, N.S., Spetter, C.V., Fernández-Severini, M.D., 2021. COVID-19 pandemic repercussions on plastic and antiviral polymeric textile causing pollution on beaches and coasts of South America. Sci. Total Environ. 763, 144365. doi:10.1016/j.scitotenv.2020.144365

Bessa, F., Kogel, T., Frias, J., Lusher, A., 2019. Harmonized protocol for monitoring microplastics in biota, Micropoll-Multilevel assessment of microplastics and associated pollutants in the Baltic Sea View project. doi:10.13140/RG.2.2.28588.72321/1

Boyle, L., 2020. Bird dies after getting tangled in coronavirus face mask | The Independent | The Independent [WWW Document]. Independent.

Brandon, J., Goldstein, M., Ohman, M.D., 2016. Long-term aging and degradation of microplastic particles: Comparing in situ oceanic and experimental weathering patterns. Mar. Pollut. Bull. 110, 299–308. doi:10.1016/j.marpolbul.2016.06.048

Bringer, A., Thomas, H., Prunier, G., Dubillot, E., Bossut, N., Churlaud, C., Clérandeau, C.,

Le Bihanic, F., Cachot, J., 2020. High density polyethylene (HDPE) microplastics impair development and swimming activity of Pacific oyster D-larvae, Crassostrea gigas, depending on particle size. Environ. Pollut. 260, 113978. doi:10.1016/j.envpol.2020.113978

Brown, W.K., Wohletz, K.H., 1995. Derivation of the Weibull distribution based on physical principles and its connection to the Rosin–Rammler and lognormal distributions. J. Appl. Phys. 78, 2758–2763. doi:10.1063/1.360073

Caputo, F., Vogel, R., Savage, J., Vella, G., Law, A., Della Camera, G., Hannon, G., Peacock, B., Mehn, D., Ponti, J., Geiss, O., Aubert, D., Prina-Mello, A., Calzolai, L., 2021. Measuring particle size distribution and mass concentration of nanoplastics and microplastics: addressing some analytical challenges in the sub-micron size range. J. Colloid Interface Sci. 588, 401–417. doi:10.1016/j.jcis.2020.12.039

Cesa, F.S., Turra, A., Checon, H.H., Leonardi, B., Baruque-Ramos, J., 2020. Laundering and textile parameters influence fibers release in household washings. Environ. Pollut. 257, 113553. doi:10.1016/j.envpol.2019.113553

Chamas, A., Moon, H., Zheng, J., Qiu, Y., Tabassum, T., Jang, J.H., Abu-Omar, M., Scott, S.L., Suh, S., 2020. Degradation Rates of Plastics in the Environment. ACS Sustain. Chem. Eng. 8, 3494–3511. doi:10.1021/acssuschemeng.9b06635

Chua, M.H., Cheng, W., Goh, S.S., Kong, J., Li, B., Lim, J.Y.C., Mao, L., Wang, S., Xue, K., Yang, L., Ye, E., Zhang, K., Cheong, W.C.D., Tan, Beng Hoon, Li, Z., Tan, Ban Hock, Loh, X.J., 2020. Face Masks in the New COVID-19 Normal: Materials, Testing, and Perspectives. Research 2020, 1–40. doi:10.34133/2020/7286735

De-la-Torre, G.E., Rakib, M.R.J., Pizarro-Ortega, C.I., Dioses-Salinas, D.C., 2021. Occurrence of personal protective equipment (PPE) associated with the COVID-19 pandemic along the coast of Lima, Peru. Sci. Total Environ. 774, 145774. doi:10.1016/j.scitotenv.2021.145774

De Falco, F., Gullo, M.P., Gentile, G., Di Pace, E., Cocca, M., Gelabert, L., Brouta-Agnésa, M., Rovira, A., Escudero, R., Villalba, R., Mossotti, R., Montarsolo, A., Gavignano, S., Tonin, C., Avella, M., 2018. Evaluation of microplastic release caused by textile washing processes of synthetic fabrics. Environ. Pollut. 236, 916–925. doi:10.1016/j.envpol.2017.10.057

Ding, Z., Babar, A.A., Wang, C., Zhang, P., Wang, X., Yu, J., Ding, B., 2020. Spunbonded needle-punched nonwoven geotextiles for filtration and drainage applications: Manufacturing and structural design. Compos. Commun. 100481. doi:10.1016/j.coco.2020.100481

Duan, J., Bolan, N., Li, Y., Ding, S., Atugoda, T., Vithanage, M., Sarkar, B., Tsang, D.C.W., Kirkham, M.B., 2021. Weathering of microplastics and interaction with other coexisting constituents in terrestrial and aquatic environments. Water Res. 196, 117011. doi:10.1016/j.watres.2021.117011

Ekvall, M.T., Lundqvist, M., Kelpsiene, E., Šileikis, E., Gunnarsson, S.B., Cedervall, T., 2019. Nanoplastics formed during the mechanical breakdown of daily-use polystyrene products. Nanoscale Adv. 1, 1055–1061. doi:10.1039/C8NA00210J

Enfrin, M., Lee, J., Gibert, Y., Basheer, F., Kong, L., Dumée, L.F., 2020. Release of hazardous nanoplastic contaminants due to microplastics fragmentation under shear stress forces. J. Hazard. Mater. 384, 121393. doi:10.1016/j.jhazmat.2019.121393

Frias, J.P.G.L., Nash, R., 2019. Microplastics: Finding a consensus on the definition. Mar. Pollut. Bull. 138, 145–147. doi:10.1016/j.marpolbul.2018.11.022

Gallo Neto, H., Gomes Bantel, C., Browning, J., Della Fina, N., Albuquerque Ballabio, T., Teles de Santana, F., de Karam e Britto, M., Beatriz Barbosa, C., 2021. Mortality of a juvenile Magellanic penguin (Spheniscus magellanicus, Spheniscidae) associated with the ingestion of a PFF-2 protective mask during the Covid-19 pandemic. Mar. Pollut. Bull. 166, 112232. doi:10.1016/j.marpolbul.2021.112232

Gigault, J., Halle, A. ter, Baudrimont, M., Pascal, P.-Y., Gauffre, F., Phi, T.-L., El Hadri, H., Grassl, B., Reynaud, S., 2018. Current opinion: What is a nanoplastic? Environ. Pollut. 235, 1030–1034. doi:10.1016/j.envpol.2018.01.024

Henry, B., Laitala, K., Klepp, I.G., n.d. Microfibres from apparel and home textiles: Prospects for including microplastics in environmental sustainability assessment. Sci. Total Environ. doi:S004896971834049X

Hernandez, E., Nowack, B., Mitrano, D.M., 2017. Polyester Textiles as a Source of Microplastics from Households: A Mechanistic Study to Understand Microfiber Release During Washing. Environ. Sci. Technol. 51, 7036–7046. doi:10.1021/acs.est.7b01750

Jiang, B., Kauffman, A.E., Li, L., McFee, W., Cai, B., Weinstein, J., Lead, J.R., Chatterjee, S., Scott, G.I., Xiao, S., 2020. Health impacts of environmental contamination of micro- and nanoplastics: a review. Environ. Health Prev. Med. 25, 29. doi:10.1186/s12199-020-00870-9

Julienne, F., Delorme, N., Lagarde, F., 2019. From macroplastics to microplastics: Role of water in the fragmentation of polyethylene. Chemosphere 236, 124409. doi:10.1016/j.chemosphere.2019.124409

Kaile, N., Lindivat, M., Elio, J., Thuestad, G., Crowley, Q.G., Hoell, I.A., 2020. Preliminary Results From Detection of Microplastics in Liquid Samples Using Flow Cytometry. Front. Mar. Sci. 7. doi:10.3389/fmars.2020.552688

Kane, I.A., Clare, M.A., Miramontes, E., Wogelius, R., Rothwell, J.J., Garreau, P., Pohl, F., 2020. Seafloor microplastic hotspots controlled by deep-sea circulation. Science (80-.). 368, 1140–1145. doi:10.1126/science.aba5899

Lambert, S., Wagner, M., 2016. Characterisation of nanoplastics during the degradation of polystyrene. Chemosphere 145, 265–268. doi:10.1016/j.chemosphere.2015.11.078

Layton, B.E., 2008. A Comparison of Energy Densities of Prevalent Energy Sources in Units of Joules Per Cubic Meter. Int. J. Green Energy 5, 438–455.

523 doi:10.1080/15435070802498036
524 Le Bihanic, F., Clérandeau, C., Cormier, B., Crebassa, J.-C., Keiter, S.H., Beiras, R., Morin,
525 B., Bégout, M.-L., Cousin, X., Cachot, J., 2020. Organic contaminants sorbed to
526 microplastics affect marine medaka fish early life stages development. Mar. Pollut. Bull.
527 154, 111059. doi:10.1016/j.marpolbul.2020.111059
528 Li, L., Zhao, X., Li, Z., Song, K., 2021. COVID-19: Performance study of microplastic
529 inhalation risk posed by wearing masks. J. Hazard. Mater. 411, 124955.
530 doi:10.1016/j.jhazmat.2020.124955
531 Mattsson, K., Björkroth, F., Karlsson, T., Hassellöv, M., 2021. Nanofragmentation of
532 Expanded Polystyrene Under Simulated Environmental Weathering (Thermooxidative
533 Degradation and Hydrodynamic Turbulence). Front. Mar. Sci. 7.
534 doi:10.3389/fmars.2020.578178
535 Monteleone, A., Brandau, L., Schary, W., Wenzel, F., 2021. Using autofluorescence for
536 microplastic detection – Heat treatment increases the autofluorescence of microplastics1.
537 Clin. Hemorheol. Microcirc. 76, 473–493. doi:10.3233/CH-209223
538 Morgana, S., Ghigliotti, L., Estévez-Calvar, N., Stifanese, R., Wieckzorek, A., Doyle, T.,
539 Christiansen, J.S., Faimali, M., Garaventa, F., 2018. Microplastics in the Arctic: A case
540 study with sub-surface water and fish samples off Northeast Greenland. Environ. Pollut.
541 242, 1078–1086. doi:10.1016/j.envpol.2018.08.001
542 Napper, I.E., Thompson, R.C., 2016. Release of synthetic microplastic plastic fibres from
543 domestic washing machines: Effects of fabric type and washing conditions. Mar. Pollut.
544 Bull. 112, 39–45. doi:10.1016/j.marpolbul.2016.09.025
545 Ó Briain, O., Marques Mendes, A.R., McCarron, S., Healy, M.G., Morrison, L., 2020. The
546 role of wet wipes and sanitary towels as a source of white microplastic fibres in the
547 marine environment. Water Res. 182, 116021. doi:10.1016/j.watres.2020.116021
548 Okuku, E., Kiteresi, L., Owato, G., Otieno, K., Mwalugha, C., Mbuche, M., Gwada, B.,

549 Nelson, A., Chepkemboi, P., Achieng, Q., Wanjeri, V., Ndwiga, J., Mulupi, L., Omire,
550 J., 2021. The impacts of COVID-19 pandemic on marine litter pollution along the
551 Kenyan Coast: A synthesis after 100 days following the first reported case in Kenya.
552 Mar. Pollut. Bull. 162, 111840. doi:10.1016/j.marpolbul.2020.111840
553 Patrício Silva, A.L., Prata, J.C., Walker, T.R., Duarte, A.C., Ouyang, W., Barcelò, D., Rocha-
554 Santos, T., 2021. Increased plastic pollution due to COVID-19 pandemic: Challenges
555 and recommendations. Chem. Eng. J. 405, 126683. doi:10.1016/j.cej.2020.126683
556 Piruska, A., Nikcevic, I., Lee, S.H., Ahn, C., Heineman, W.R., Limbach, P.A., Seliskar, C.J.,
557 2005. The autofluorescence of plastic materials and chips measured under laser
558 irradiation. Lab Chip 5, 1348. doi:10.1039/b508288a
559 Prata, J.C., Reis, V., da Costa, J.P., Mouneyrac, C., Duarte, A.C., Rocha-Santos, T., 2021.
560 Contamination issues as a challenge in quality control and quality assurance in
561 microplastics analytics. J. Hazard. Mater. 403, 123660.
562 doi:10.1016/j.jhazmat.2020.123660
563 Prata, J. C., Silva, A. L. P., Duarte, A. C., Rocha-Santos, T. 2021. Disposable over Reusable
564 Face Masks: Public Safety or Environmental Disaster?. Environments, 8(4), 31.
565 doi:10.3390/environments8040031
566 Ragazzi, M., Rada, E.C., Schiavon, M., 2020. Municipal solid waste management during the
567 SARS-COV-2 outbreak and lockdown ease: Lessons from Italy. Sci. Total Environ. 745,
568 141159. doi:10.1016/j.scitotenv.2020.141159
569 Saadat, S., Rawtani, D., Hussain, C.M., 2020. Environmental perspective of COVID-19. Sci.
570 Total Environ. 728, 138870. doi:10.1016/j.scitotenv.2020.138870
571 Saliu, F., Veronelli, M., Raguso, C., Barana, D., Galli, P., Lasagni, M., 2021. The release
572 process of microfibers: from surgical face masks into the marine environment. Environ.
573 Adv. 4, 100042. doi:10.1016/j.envadv.2021.100042
574 Sathicq, M.B., Sabatino, R., Corno, G., Di Cesare, A., 2021. Are microplastic particles a

hotspot for the spread and the persistence of antibiotic resistance in aquatic systems? Environ. Pollut. 279, 116896. doi:10.1016/j.envpol.2021.116896

Shackelford, J.F., 2000. Materials science for engineers, Upper Saddle River. New Jersey.

Shruti, V.C., Pérez-Guevara, F., Elizalde-Martínez, I., Kutralam-Muniasamy, G., 2020. Reusable masks for COVID-19: A missing piece of the microplastic problem during the global health crisis. Mar. Pollut. Bull. 161, 111777. doi:10.1016/j.marpolbul.2020.111777

Singh, N., Tiwari, E., Khandelwal, N., Darbha, G.K., 2019. Understanding the stability of nanoplastics in aqueous environments: effect of ionic strength, temperature, dissolved organic matter, clay, and heavy metals. Environ. Sci. Nano 6, 2968–2976. doi:10.1039/C9EN00557A

Song, Y.K., Hong, S.H., Jang, M., Han, G.M., Jung, S.W., Shim, W.J., 2017. Combined Effects of UV Exposure Duration and Mechanical Abrasion on Microplastic Fragmentation by Polymer Type. Environ. Sci. Technol. 51, 4368–4376. doi:10.1021/acs.est.6b06155

Sullivan, G.L., Delgado-Gallardo, J., Watson, T.M., Sarp, S., 2021. An investigation into the leaching of micro and nano particles and chemical pollutants from disposable face masks - linked to the COVID-19 pandemic. Water Res. 196, 117033. doi:10.1016/j.watres.2021.117033

Timár, G., Blömer, J., Kun, F., Herrmann, H.J., 2010. New Universality Class for the Fragmentation of Plastic Materials. Phys. Rev. Lett. 104, 095502. doi:10.1103/PhysRevLett.104.095502

Vethaak, A.D., Leslie, H.A., 2016. Plastic Debris Is a Human Health Issue. Environ. Sci. Technol. 50, 6825–6826. doi:10.1021/acs.est.6b02569

Wesch, C., Elert, A.M., Wörner, M., Braun, U., Klein, R., Paulus, M., 2017. Assuring quality in microplastic monitoring: About the value of clean-air devices as essentials for verified

data. Sci. Rep. 7, 5424. doi:10.1038/s41598-017-05838-4

World Health Organization, 2020. Shortage of personal protective equipment endangering health workers worldwide. World Heal. Organ.

Wu, H., Huang, J., Zhang, C.J.P., He, Z., Ming, W.-K., 2020. Facemask shortage and the novel coronavirus disease (COVID-19) outbreak: Reflections on public health measures. EClinicalMedicine 21, 100329. doi:10.1016/j.eclinm.2020.100329

Xu, E.G., Ren, Z.J., 2021. Preventing masks from becoming the next plastic problem. Front. Environ. Sci. Eng. 15, 125. doi:10.1007/s11783-021-1413-7

Yang, L., Qiao, F., Lei, K., Li, H., Kang, Y., Cui, S., An, L., 2019. Microfiber release from different fabrics during washing. Environ. Pollut. 249, 136–143. doi:10.1016/j.envpol.2019.03.011

Young, E.W.K., Berthier, E., Beebe, D.J., 2013. Assessment of Enhanced Autofluorescence and Impact on Cell Microscopy for Microfabricated Thermoplastic Devices. Anal. Chem. 85, 44–49. doi:10.1021/ac3034773

Zambrano-Monserrate, M.A., Ruano, M.A., Sanchez-Alcalde, L., 2020. Indirect effects of COVID-19 on the environment. Sci. Total Environ. 728, 138813. doi:10.1016/j.scitotenv.2020.138813

Zambrano, M.C., Pawlak, J.J., Daystar, J., Ankeny, M., Cheng, J.J., Venditti, R.A., 2019. Microfibers generated from the laundering of cotton, rayon and polyester based fabrics and their aquatic biodegradation. Mar. Pollut. Bull. 142, 394–407. doi:10.1016/j.marpolbul.2019.02.062

Zhang, K., Hamidian, A.H., Tubić, A., Zhang, Y., Fang, J.K.H., Wu, C., Lam, P.K.S., 2021. Understanding plastic degradation and microplastic formation in the environment: A review. Environ. Pollut. 274, 116554. doi:10.1016/j.envpol.2021.116554

Zhang, M., Xu, L., 2020. Transport of micro- and nanoplastics in the environment: Trojan-Horse effect for organic contaminants. Crit. Rev. Environ. Sci. Technol. 1–37.

627 doi:10.1080/10643389.2020.1845531

628

Table 1. Effects of shear stress intensity (i.e., treatment time and shear power) on fabric texture damage, water temperature (°C), and fabric deterioration (% of weight loss). Mean values (± standard deviation of triplicates) are reported.

Shear time (s)	Energy density (kJ/L)	Water T (°C)	Weight loss (mg)	Fabric deterioration (%)
1	1.6	17.5	1.0 ± 1.6	0.2 ± 0.3
15	24.0	18.0	1.6 ± 1.0	0.3 ± 0.1
30	48.0	18.2	3.0 ± 0.2	0.6 ± 0.1
60*	96.0	19.1	11.2 ± 7.3	2.1 ± 1.4
120	192.0	21.0	15.6 ± 12.3	3.2 ± 2.7

* 4 replicates.

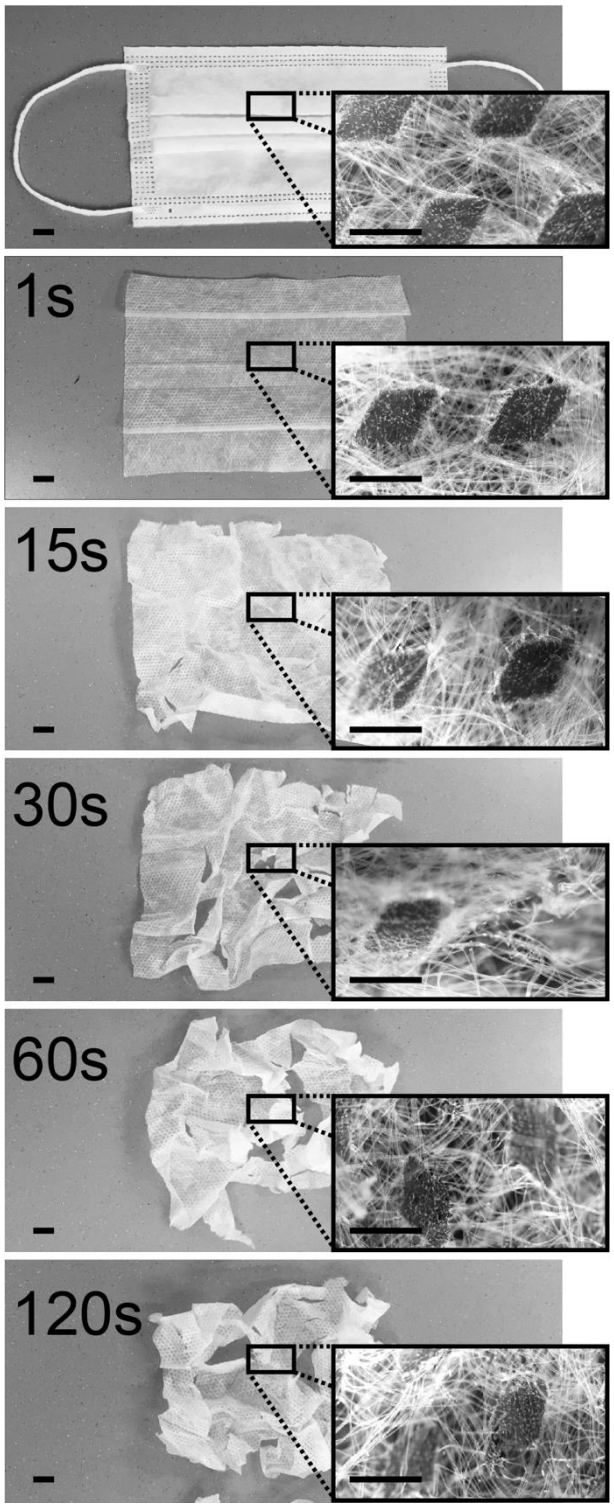

Figure 1. Deterioration of PP fabric excised from a face mask at increasing treatment time (from 1s to 120 s) and shear stress intensities (from 1.6 kJ/L to 192.0 kJ/L) (scale bar = 10 mm). 40× Microscopic images (black boxes) show the intact and progressively damaged fabric texture (scale bar = 1 mm).

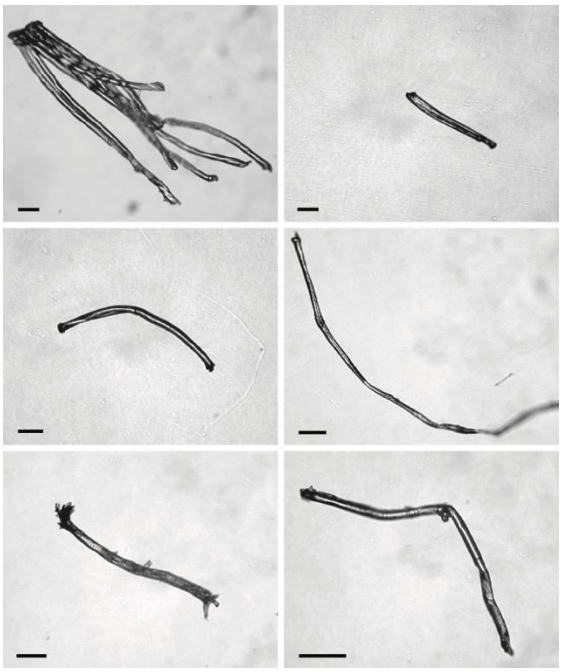

Figure 2. Selected images of microplastic fragments and fibers excised from the PP filament web of the face mask fabric and released in water during the shear tests (scale bar = 0.1 mm).

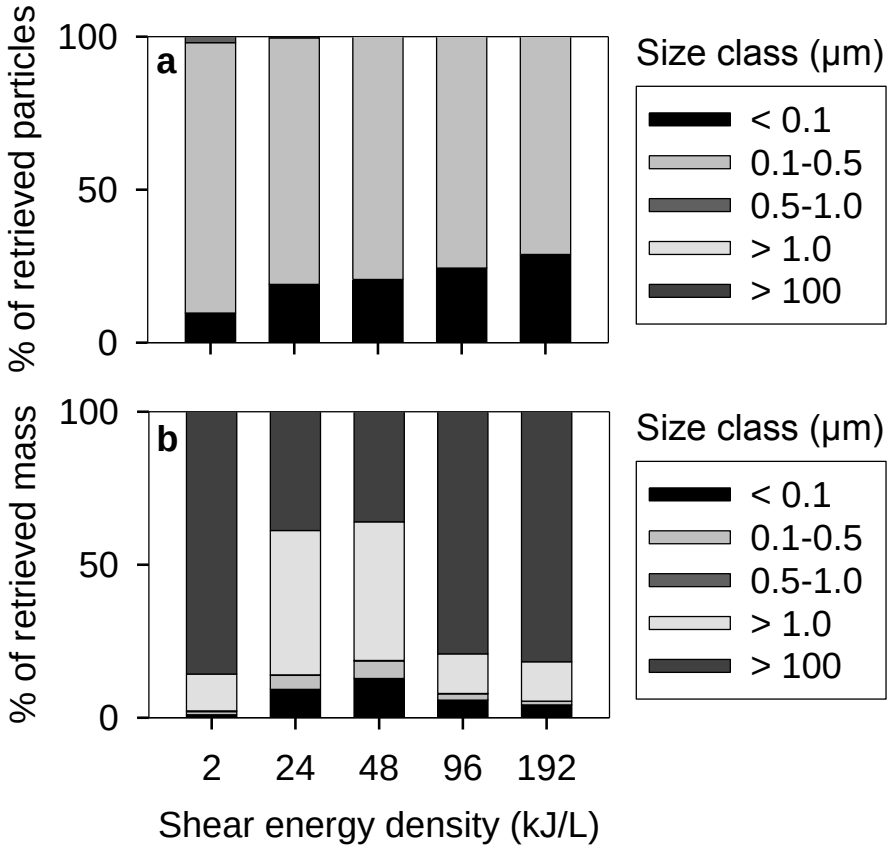

644

645 **Figure 3**. Relative contribution to total number (a) and mass (b) of detected

646 micro/nanoplastics released in water during the shear tests. Conversion in weight was based

647 on particle morphology and mean size within the 5 size classes.

648

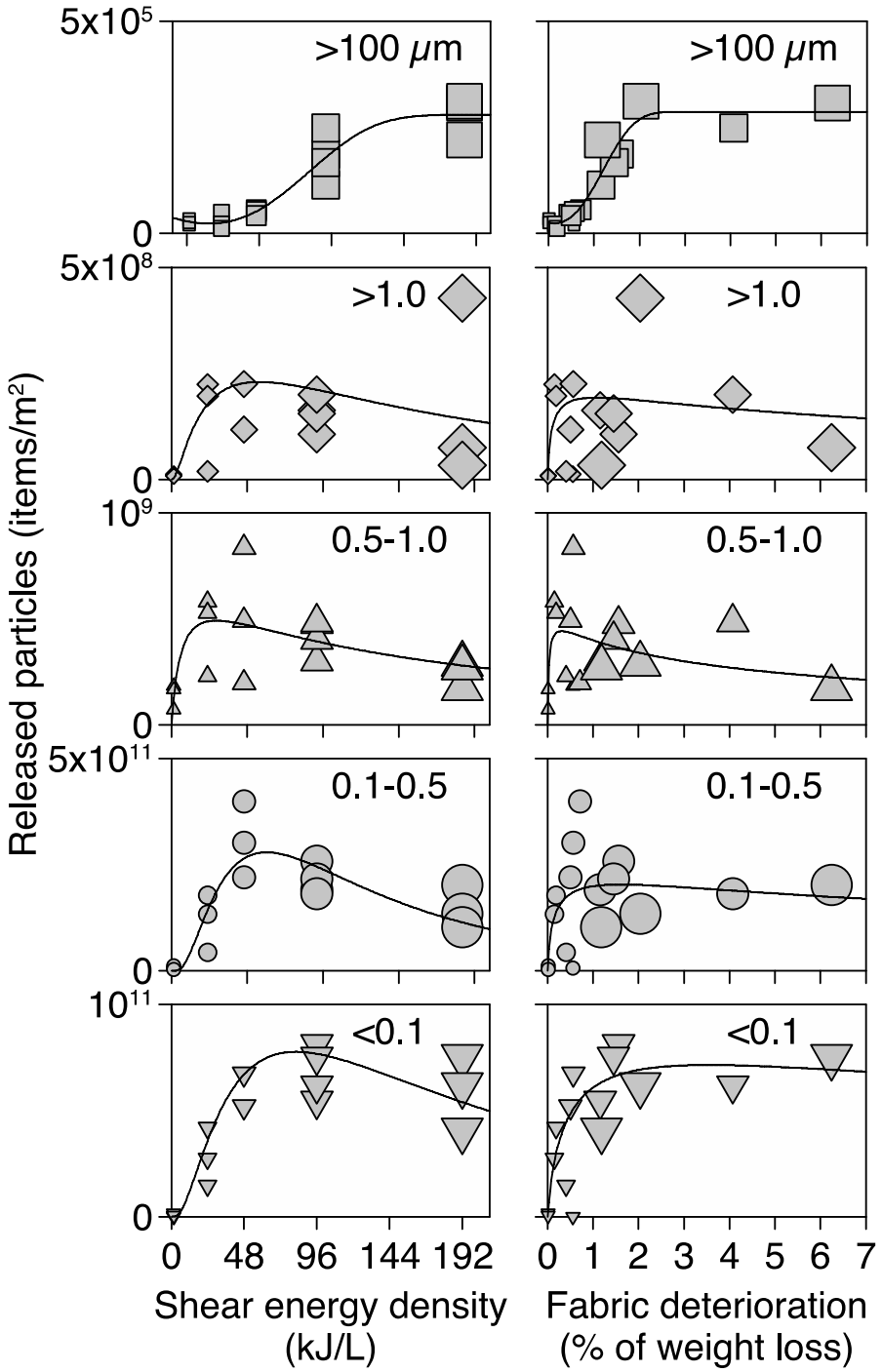

649

650

651 **Figure 4**. Patterns of particle release from face mask fabric in water at increasing shear stress
652 and fabric deterioration. Symbol size increases with treatment time. Sigmoid Weibull and
653 lognormal distributions were applied to model the occurrence of particles within the 5 size
654 classes.

655

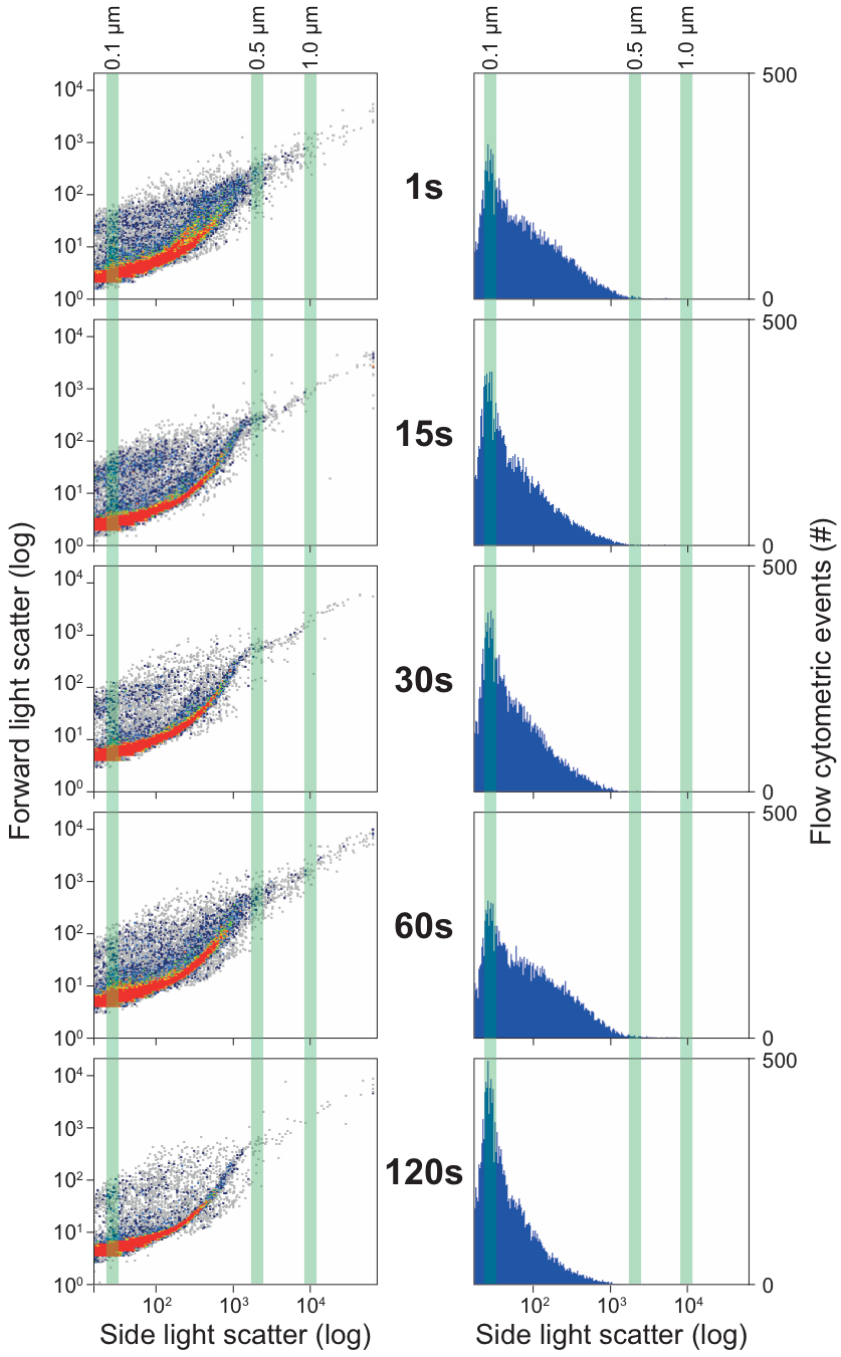

Figure S1. Micro/nanoplastic particles released from face mask fabrics and detected by flow cytometry at increasing shear times. Specific gates onto log-scaled density plots of side vs forward scatter signals (left panels) and histogram plots (right panels) were designed using the reference size of calibration beads. Accordingly, we identified the classes "> 1.0" (MPs with a nominal diameter ≥ 1.0 µm but smaller than then maximum analytical size of 100 µm), "0.5-1.0" (NPs ≥ 0.5 µm but < 1 µm), "0.1-0.5" (NPs ≥ 0.1 µm but < 0.5 µm), "< 0.1" (NPs < 0.1 µm but larger than then minimum analytical size).